Genetic, epigenetic and microbiome characterisation of an earthworm species (Octolasion lacteum) along a radiation exposure gradient at Chernobyl

Newbold, L. K., Robinson, A., Rasnaca, I., Lahive, E., Gweon, H. S. ORCID: https://orcid.org/0000-0002-6218-6301, Lapied, E., Oughton, D., Gashchak, S., Beresford, N. A. and Spurgeon, D. J. (2019) Genetic, epigenetic and microbiome characterisation of an earthworm species (Octolasion lacteum) along a radiation exposure gradient at Chernobyl. Environmental Pollution, 255 (Part 1). 113238. ISSN 0269-7491 doi: 10.1016/j.envpol.2019.113238 Available at https://centaur.reading.ac.uk/87026/

Published version at: http://dx.doi.org/10.1016/j.envpol.2019.113238
To link to this article DOI: http://dx.doi.org/10.1016/j.envpol.2019.113238

Publisher: Elsevier

Genetic, epigenetic and microbiome characterisation of an earthworm species (*Octolasion lacteum*) along a radiation exposure gradient at Chernobyl

Newbold, Lindsay K. [a *], Robinson, Alex [a *], Rasnaca, I. [a], Lahive, Elma. [a], Gweon, H. Soon [a,b], Lapied, Emmanuel [c], Oughton, Deborah [c], Gashchak, Sergey [d], Beresford, Nicholas A. [e], Spurgeon, David J. [a,†].

[a] Centre for Ecology and Hydrology, MacLean Building, Benson Lane, Wallingford, Oxon, OX10 8BB, UK.

[b] School of Biological Sciences, University of Reading, Whiteknights, Reading, Berkshire, RG6 6AH, UK.

[c] Centre for Environmental Radioactviity, Norwegian University of Life Science, 1430 Aas, Norway

[d] Chornobyl Center for Nuclear Safety, Radioactive Waste and Radioecology, Slavutych, Kiev Region, Ukraine

[e] NERC Centre for Ecology & Hydrology, Lancaster Environment Center, Library Av., Bailrigg, Lancaster LA14AP, UK

[*] The authors contributed equally to this work

[†] Author to whom correspondence should be addressed David Spurgeon, Centre for Ecology and Hydrology, MacLean Building, Benson Lane, Wallingford, Oxon, OX10 8BB, UK. email: dasp@ceh.ac.uk

Abstract

The effects of exposure to different levels of ionising radiation were assessed on the genetic, epigenetic and microbiome characteristics of the "hologenome" of earthworms collected at sites within the Chernobyl exclusion zone (CEZ). The earthworms *Aporrectodea caliginosa* (Savigny, 1826) and *Octolasion lacteum* (Örley, 1881) were the two species that were most frequently found at visited sites, however, only *O. lacteum* was present at sufficient number across different exposure levels to enable comparative hologenome analysis. The identification of morphotype *O. lacteum* as a probable single clade was established using a combination of mitochondrial (cytochrome oxidase I) and nuclear genome (Amplified Fragment Length Polymorphism (AFLP) using *Msp*I loci). No clear site associated differences in population genetic structure was found between populations using the AFLP marker loci. Further, no relationship between ionising radiation exposure levels and the percentage of methylated loci or pattern of distribution of DNA methylation marks was found. Microbiome structure was clearly site dependent, with gut microbiome community structure and diversity being systematically associated with calculated site-specific earthworm dose rates. There was, however, also co-correlation between earthworm dose rates and other soil properties, notably soil pH; a property known to affect soil bacterial community structure. Such co-correlation means that it is not possible to attribute microbiome changes unequivocally to radionuclide exposure. A better understanding of the relationship between radionuclide exposure soil properties and their interactions on bacterial microbiome community response is, therefore, needed to establish whether these the observed microbiome changes are attributed directly to radiation exposure, other soil properties or to an interaction between multiple variables at sites within the CEZ.

Capsule: Selected earthworm hologenome traits (e.g. gut microbiome) are potentially influenced by radiation exposure, but also confounding soil property variables

Keywords: Radioecology, ^{137}Caesium, Earthworm, DNA methylation, Microbiome,

Introduction

The Chernobyl nuclear accident on April 26th 1986 was responsible for a large-scale release of radionuclides into the surrounding ecosystem, resulting in long-term exposure of the local and wider environment. Exposure to radioactivity in controlled, high dose laboratory studies has been shown to have effects on soil invertebrate species including earthworms (Hertel-Aas et al., 2007; Rusin et al., 2019; Sowmithra et al., 2015), springtails (Nakamori et al., 2008) and nematodes (Dubois et al., 2019; Lecomte-Pradines et al., 2017). Further, research on the long-term effects of ionising radiation in the surrounds of the former power station, now known as the Chernobyl Exclusion Zone or CEZ, have provided information on the physiological and ecological responses of individuals, populations and ecosystems to chronic radiation exposure (see Beresford et al., 2016; Geras'kin et al., 2008; Hinton et al., 2007; Lourenco et al., 2016). Despite these studies, there is a lack of consensus on the long-term effects of radiation on wildlife in the CEZ, with some studies suggesting wide-scale impacts and others limited effects (Beresford et al., 2019b). Further work is, therefore, needed to understand how radiation exposure affected soil organisms, especially under long-term chronic exposure scenarios.

The soil was one of the main sinks for radionuclides released by the Chernobyl accident. The initially high levels in CEZ soils were shown to alter soil invertebrate population sizes and community structure (Krivolutsky, 1996). For example, reduced recruitment rates of the earthworms *Aporrectodea caliginosa and Dendrobaena octaedra* (Savigny, 1826) resulted in a population decline in contaminated forest sites (Krivolutzkii et al., 1992). Over time, however, earthworm populations at sites in the CEZ showed some recovery, such that within 3 years of the accident, immature/adult ratios and overall earthworm biomass in the previously impacted sites no longer differed from that in uncontaminated areas (Krivolutsky, 1996). Despite this rebound, species diversity has, however, remained lower at some sites (Geras'kin et al., 2008). This initial decline and recovery of earthworm populations in the CEZ in response to acute exposure may provide only a limited picture of potential response trajectory of earthworms to exposure which may also encompass chronic effects on traits relevant for long-term individual physiology and

84 population dynamics. For example, in a review of the impacts of the 1957 Kyshtym (Russian
85 Urals) accident, reports indicate that soil invertebrate communities had not been restored at a
86 contaminated site (the main contaminant being 90Sr) c. 30 years after the accident (see Zaitsev
87 et al., 2014). Given the low dispersal rates (e.g. of the order of 5-10 m a-1 for earthworms which
88 may limit recolonization potential (Marinissen and Vandenbosch, 1992), such a long-term impact
89 of an acute radiation event would seem plausible.
90
91 The decline and potentially ongoing change for earthworm populations observed at some CEZ
92 sites in the aftermath of the accident raises fundamental questions regarding the potentially
93 adaptive mechanisms by which these organisms may respond to ongoing chronic exposure (as
94 reviewed by Geras'kin et al., 2008). One possibility may lie in population recovery from a low
95 starting density as exposure abates through radioactive decay and radionuclide transport to
96 deeper soil layers. However, even within this scenario, the selection of tolerant individuals leading
97 to the development of an adapted population may also play a role. At Chernobyl, both plant and
98 fungal species have been shown to develop tolerance to radioisotope exposures (Boubriak et al.,
99 2008; Egorova et al., 2015). However, despite evidence for the development of tolerance in
100 earthworms to other pollutants (Fisker et al., 2013; Kille et al., 2013; Langdon et al., 2003), genetic
101 adaptation to radionuclide exposure in this taxa has yet to be clearly established. Adaptation to
102 adverse conditions can result both from phenotypic plastic responses, such as changes in gene
103 expression mediated through modifications in the epigenetic gene regulation, as well as more
104 classically through the selection of traits associated with tolerance. Additionally, changes in the
105 structure and associated function of the host-microbiome can also play a role (Pass et al., 2015).
106
107 The concept of the “hologenome” recognises that changes in the regulation/activity of the genes
108 of the organism itself *and* changes in the community and functional activity of mutualistic
109 (microbial) communities can in combination contribute to the overall development of adapted
110 phenotypes (Bordenstein and Theis, 2015). To assess how different components of the
111 hologenome respond to radiological exposure (and other environmental co-variables), we here

measure genetic, epigenetic and gut microbiome changes occurring in earthworms (predominantly *Octolasion lacteum*) collected from multiple sites along a contamination gradient in the CEZ. Genetic trait analysis was undertaken using cytochrome oxidase 1 (COI) sequencing and the measurement of nuclear sequence polymorphisms using AFLP analysis using one restriction enzyme, epigenetic traits were assessed by DNA methylation profiling using methylation sensitive AFLP (meAFLP) conducted by comparing the first AFLP profile to those obtained using a second DNA methylation sensitive restriction enzyme. Gut microbiome structure was quantified using 16S rRNA loci sequencing. These analyses allow us to test the hypothesis that different genetic, epigenetic and microbiome traits of the hologenome show radiation exposure level dependent changes.

123 ***Materials and methods***

124 An pilot field trip to the Chernobyl Exclusion Zone (CEZ) was carried out in October 2014 to identify
125 the earthworm species present within the zone. Twenty sites representing dominant habitats
126 (grasslands, woodlands, wetlands) were visited. Qualitative sampling collected earthworms from
127 a 50 m x 50 m area over a 2 h search period. This initial survey indicated that earthworms are
128 relatively uncommon in the CEZ. Indeed, many sites lack this taxon. This limited distribution is
129 likely due mainly to the sandy, low pH, low organic matter nature of the soils present, which are
130 known to be unfavourable for earthworms (Edwards, 2004; Ouellet et al., 2008). Where
131 earthworms were found, they were usually associated with the margins of water bodies,
132 marshlands or in improved soils, such as the gardens of abandoned communities. Based on this
133 information, a second field trip was carried out in October 2016 to collect earthworms of one or
134 more species systematically from sites ranging in expected radionuclide exposure from
135 background to relatively high, with wetlands identified as the main habitats for sampling.
136
137 During the second field campaign, six earthworm species, *Eiseniella tetraedra* (Savigny, 1826),
138 *Eisenia fetida* (Savigny, 1826), *O. lacteum*, *Lumbricus rubellus* (Hoffmeister, 1843), *A. caliginosa*
139 and *Aporrectodea rosea* (Savigny, 1826) were found at nine sampled sites. Three of these species
140 (*E. fetida*, *L. rubellus* and *A. rosea*) were collected from a limited number of sites giving insufficient
141 variation in radioactivity exposure for the collected specimens. Although *E. tetraedra* was collected
142 from five sites that covered different radioactivity exposure levels, densities were very low limiting
143 statistical power. Only, *O. lacteum* was found in sufficient, although sometimes at low, numbers
144 across multiple sites with measured and modeled radiation exposure levels ranging from
145 background to high. Therefore, this species has been selected for the genetic, epigenetic and
146 microbiome trait analyses. It should, however, be noted that due to challenges in distinguishing
147 between species based only upon morphology, additional genetic marker analysis was applied to
148 a further earthworm species (*A. caliginosa*) in order to corroborate in field taxonomic identity. At
149 each site, effort was made to collect multiple individuals per site within the restricted timeframe
150 (as Governed by access permissions) that was available for collection. This was often challenging

as even at sites where earthworms were present, densities were often low. Each individual collected was treated thereafter as a separate biological replicate for that sample location.

Live earthworms were collected from the soil by digging and hand sorting. Individuals were maintained on own site soil for transfer to a local working area for identification and subsequent dissection for tissue samples. Due to the unique conditions presented by the sample site (remote location, sampling period limitations, and minimal facilities) an on-site protocol was used for sampling and tissue preservation. All earthworms were initially weighed, surface cleaned in phosphate-buffered saline to remove any adhering soil particles. The position of the worm's clitellum was used to divide the tissue into anterior (including the clitellum) and posterior section samples. To preserve sample integrity, tissues intended for later DNA extraction were cut into small pieces and placed in 1:10 ratio of sample weight to DNA/RNA shield™ lysis and preservation buffer (Zymo Research, Irvine, USA). Samples were lysed in the field using the super FastPrep™ handheld homogenizer and Lysing Matrix E (both from MP Biomedicals, Eschwege, Germany). Lysed samples and sampled soils (to 10 cm depth) were transported back to the main laboratory and stored at -20°C prior to DNA extraction. The soils sampled at each site were also used for radionuclide (Cs-137, Sr-90, Am-241, Pu-total isotope) activity measurements for dosimetry calculation. This augmented the simple measurement of air dose rate made *in-situ* at each site.

Radionuclide Measurement and dosimetry approach

Soil and earthworm ^{137}Cs concentrations were measured using gamma spectrometry (Ge and NaI scintillation detectors, Canberra). Whole earthworm and earthworm soil gut measurements of ^{137}Cs were carried out when samples were available. Soil ^{90}Sr concentrations were determined using beta spectrometry of the daughter nuclide ^{90}Y, and ^{241}Am using low energy gamma spectrometry. Pu concentrations (total Pu-isotopes: ^{238}Pu, ^{239}Pu, ^{240}Pu) were determined after sample dissolution (65% HNO_3), anion exchange separation (BioRad AG 1 × 8, 100–200 mesh) and co-precipitation using ^{242}Pu added as a yield tracer. These samples were then counted using

a planar ion implanted silicon detector. All methods were calibrated against standards and counting errors were typically <3% for ^{90}Sr, <7% for ^{137}Cs and <20% for the Pu isotopes.

Controversies in interpreting results from field-based radioecology studies can arise due to an incomplete assessment of actual organism exposure (Bonzom et al., 2016). Thus, while external dose rates can provide an indication of exposure at sites, they usually underestimate actual doses received by an organism, since they do not include the contribution from internalised radionuclides. Therefore, we chose to estimate exposure as weight absorbed dose rate, which includes the contribution of all radiation types (alpha, beta and gamma emitters) from all exposure pathways (internal and external), as opposed to just ambient external dose rates measured with dosimeters (e.g. Moller and Mousseau, 2009; Uematsu et al., 2015). The approach to dosimetry assessment for all sites used a stepwise approach that: 1) recorded air dose rates and ranges (mGy/hr) at the soil surface and 1 m above ground at each collection sites; and 2) used the measured activity levels in soils to estimate the relative internal and external dose rate contributions of each radionuclide to earthworm exposure. Dosimetry modelling was carried out within a tier 3 assessment using the ERICA tool, a software system that has a structure based upon the tiered approach to assessing the radiological risk to terrestrial, freshwater and marine biota (Brown et al., 2008), using the creation of organisms (different earthworm sizes) and site-specific data. Measured tissue concentrations of ^{137}Cs were used to calculate internal dose rates, while the ERICA default transfer ratios for earthworms were used for the other radionuclides (Popic et al., 2012). Weighting factors of 1, 3 and 10 were used for gamma and beta > 10 keV, beta < 10 keV and alpha radiation, respectively. Based on the radionuclide concentration in soil and the sampled organism, external and internal dose rates ($\mu Gy\ h^{-1}$) were calculated and used to determine total weight absorbed dose rates.

DNA extraction

Following sample return to the main research laboratory, a protocol was developed which enabled the co-extraction of the earthworm and microbial DNA from the tissue and gut microbiome

samples. Preserved tissue lysate was extracted using the Zymo research ZR-96 soil microbe DNA kit™, with the following modifications. Prior to DNA extraction samples were thawed, then incubated with 2 µl proteinase K (Promega) for 1 hour at 20ºC. All samples underwent a further mechanical lysis step on a fast prep 24 (MP Biomedicals) at 5 k for 30 sec. Lysed samples were centrifuged at 2100 *g* for 5 minutes and 250 µl of lysate combined with 750 µl soil binding buffer. All further steps were carried out according to manufacturer's protocol. Anterior (head) and posterior (tail) samples were extracted separately for analysis of earthworm genomic and microbiome traits, respectively. Large worms often contained more tail tissue than optimal for each lysis tube, where this was the case, the available tissue was spread across a number of tubes, from all of which DNA was extracted. To ensure that the entire microbiome was represented accurately, the results from all assessment for each individual worm were pooled.

Genotyping

DNA samples extracted from the body wall from the anterior proportion of the earthworm were used for the corroboration of field species identification. Approximately 20 ng of DNA template was used to amplify ~710 bp region of the mitochondrial cytochrome oxidase subunit I (COI) gene, in a 50 µl total reaction, following the addition of; 0.4 µl of taq polymerase (Sigma), 1 µl of 10 µM dNTP mix (Bioline), 0.5 µl bovine serum albumin (New England Biolabs), and 0.5 µl of 100 µM primers LCOI1490F and HC02198R (Folmer et al., 1994). Amplification conditions were as follows: 95 ºC for 2 min, then 35 cycles of 95 ºC for 1min., 40 ºC for 1 min, and 72 ºC for 1:30 min, with a final extension at 72 ºC of 10 min. PCR products were electrophoretically analysed and then purified using the ZR-96 DNA Clean-up kit™ (Zymo research). Purified PCR product was diluted at a 1:10 ratio and 1 µl used separate F and R sequencing reaction carried out using 1 µl BigDye™ terminator V 3.1 reaction mix (Applied Biosystems, USA), 1.5 µl BigDye™ terminator V 3.1 buffer, 1 µl of 3.2 µM primer solution, on an Applied Biosystems 3730 genetic analyser. Because of inconsistent amplification using LCOI1490F and HC02198R, a custom additional internal sequencing primer was designed and included for this study COI_lumbricF_seq (5'-TACAGCCACGCATTCGTTA-3'). Sequencing reactions were purified using Big Dye®

Xterminator™ purification kit (Applied Biosystems, USA) and sequenced using ABI PRISM® BigDye v3.1 Terminator technology (Applied Biosystems). Resultant sequences were base called, quality checked and assembled using Sequencher V. To act as suitable phylogenetic outgroups resultant contigs were aligned using ClustalW with reference COI sequences sourced from the barcode of life (BOLD) database, NCBI genebank and unpublished reference sequences from native worms sourced in UK (OS1). Optimal likelihood settings were determined to be TVM+G through the implementation of the Akaike Information Criterion in JModelTest V2.17 (Darriba et al., 2012; Posada, 2008). PAUP4b8 was used to generate a Neighbour Joining (NJ) tree using the likelihood criterion (with optimal settings), and bootstrap support values for 1000 replicates. The resultant tree (OS2) was used to determine the taxonomic affiliation of each earthworm and identities corroborated via inclusion in the nearest supported cluster. For *O. lacteum*, a set of successfully amplified product sequences clustered with *O. lacteum* COI sequences available from BOLD within the constructed phylogenetic tree, supporting the morphological identification for these individuals. For a remaining set of *O. lacteum* individuals (38 of 72 individuals), amplification of the COI gene failed, despite best efforts to optimize template, primers and reaction conditions for PCR. Hence, support for the morphospecies identification for these individuals was not achieved through COI sequencing. For these samples a combination of onsite morphological taxonomy and distinct species separation through AFLP profile (see Supplementary Fig. 1) was used to verify species identity.

Microbiome characterisation

Approximately 20-30 ng of template DNA collected from samples was amplified using Q5 High Fidelity Polymerase (New England Biolabs, Hitchin, UK), each sample reaction include a unique barcode-primer combination to allow separation of sequences associated with the different individuals (Kozich et al., 2013). Amplification conditions consisted of 25 cycles of an initial 30s, a 98ºC denaturation step, followed by annealing phase of 30s at 53ºC, and a final extension step lasting 90 sec at 72ºC. Primer sequence was based on the universal bacterial primer sequence combination 341F and 806R, producing amplicons of ~550 bp spanning the V3-V4 hypervariable

262 regions of the 16S small subunit ribosomal RNA gene (herein, 16S rRNA gene). PCR Products
263 were normailsed using Sequalprep normalisation plates (Invitrogen, Carlsbad, CA, USA) and the
264 resultant amplicon library was sequenced at a concentration of 5.4 pM with a 0.6 pM addition of
265 Illumina generated PhiX control library. Sequencing was performed on an Illumina MiSeq platform
266 using V3 chemistry (Illumina Inc., San Diego, CA, USA).
267
268 Sequenced paired-end reads were joined using VSEARCH (Rognes et al., 2016), quality filtered
269 using FASTX tools (hannonlab.cshl.edu), length filtered with the minimum length of 300 bp,
270 presence of PhiX and adapters were checked and removed with BBTools (jgi.doe.gov/data-and-
271 tools/bbtools/), and chimeras were identified and removed with VSEARCH_UCHIME_REF
272 (Rognes et al., 2016) using Greengenes Release 13_5 (at 97%) (DeSantis et al., 2006). Singletons
273 were removed and the resulting sequences were clustered into operational taxonomic units
274 (OTUs) with VSEARCH_CLUSTER (Rognes et al., 2016) at 97% sequence identity (Tindall et al.,
275 2010). Representative sequences for each OTU were taxonomically assigned by RDP Classifier
276 with the bootstrap threshold of 0.8 or greater (Wang et al., 2007) using Greengenes Release 13_5
277 (full) (DeSantis et al., 2006) as the reference. Unless stated otherwise, default parameters were
278 used for the steps listed. The raw sequence data reported in this study have been deposited in
279 the European Nucleotide Archive under accession number ERS3594341-ERS3594509.
280
281 After quality filtering a total of 13725096 sequences were rarefied to an even depth within the
282 phyloseq package (McMurdie and Holmes, 2013). To visualise the relationship between Miseq
283 community profiles from differing sample sites, nonmetric multidimensional scaling (NMDS) was
284 performed using the ‘ordinate’ function, based on dissimilarities calculated using the Bray–Curtis
285 index. Changes in bacterial diversity related to mean dosage were assessed using Fishers log
286 series [alpha], as this is largely unaffected by sample size and independent if individuals (N)
287 >1000. Diversity was analysed in relation to potential environmental drivers relevant for sites in
288 the CEZ including soil pH, loss on ignition and the calculated dose rates.
289

Genetic and epigenetic characterisation using dual restriction enzyme AFLP

A dual restriction enzyme based meAFLP protocol was optimised to assess genetic markers and DNA methylation at these sites. The protocol used is based on parallel use of methylation- and non-methylation-sensitive restriction enzymes (*Hpa*II and *Msp*I) to treat DNA samples prior to primer ligation and amplification (Xiong et al., 1999). Initially extracted genomic DNA is digested with *Eco*RI and then there is a second digestion step conducted for an aliquot of this sample using either the restriction enzymes *Msp*I or *Hpa*II. Both *Hpa*II and *Msp*I recognize a CCGG sequence. *Msp*I is able to cut methylated recognition sites (as well as unmethylated ones) thereby providing an assessment of relevant genetic polymorphism. In contrast, *Hpa*II is unable to cut at such locations when they are methylated (i.e. only unmethylated recognition sites are cut) which by comparing to *Msp*I profiles provides an assessment of epigenetic DNA methylation status.

The meAFLP analysis was conducted in duplicate for all *O. lacteum* and *A. caliginosa* using selective primers for the PCR reactions and analysis on an Applied Biosystems 3130 analyser (Andre et al., 2010). The presence or absence of fragments was scored on chromatograms using GeneMapper Genotyping Software 1.5. Profile bin widths were checked and manually adjusted to encompass all detected peaks. To differentiate signal from background, a Fluorescence Unit (FU) threshold of 40 units was used for a presence/absence binary matrix. All peaks were manually checked for inclusion in analysis. Rare alleles differing only in one individual were initially deleted from the data set. The total number of loci included in the analysis was 202. Fragments were scored as follows: non-methylated state if present in both *Eco*RI-*Hpa*II and *Eco*RI-*Msp*I products (1/1); methylated state if present in either *Eco*RI-*Hpa*II (1/0) or *Eco*RI-*Msp*I (0/1) products (either internal cytosine methylation (0/1) or hemimethylation (1/0)) or absent (0/0). Fragments were classified as “methylation-susceptible loci” if the observed proportion of methylated scores (1/0, 0/1 and 0/0) and “non-methylation fragments”. Principal coordinates (PCO) analysis was also used to visualise the genetic relationship between individuals using GenAlEx ver 6.4.1 (Srut et al., 2017). Site and also potential earthworm strain effects were assessed using the site principal component scores (PCoA1 and PCoA 2) after verification for normality using the Kolmogorov–

318 Smirnov test. Tests were conducted using ANOVA with site and potential strain differences as
319 factors.

Results

Earthworm distribution, collection and identification by COI barcoding

Morphotype *O. lacteum* were collected in sufficient numbers (≥3 individuals per site) across five sites covering measured surface dose rates from 0.12 - 12 µGy/h. All sampled locations yielding *O. lacteum* were associated with wetland or marshland habitats (Table 1). Morphotype *A. caliginosa* were collected from three sites covering dose rates from 0.12 - 8 µGy/h. However, all but one earthworm came from sites with exposure levels <0.2 µGy/h. This one *A. caliginosa* collected at site M2: Forest Lake 2 was the only individual to co-occur with *O. lacteum*, indicating an almost completed segregation of the two species across visited sites in the CEZ (Table 1).

To confirm the field based morphological identifications, COI gene sequencing was conducted for all individuals to provide a mitochondrial genotype for comparison with previously published sequences for the two species. For the morphotype *A. caliginosa*, the phylogenetic analysis indicated that all amplified sequences clustered with the *A. caliginosa* COI sequences available in the BOLD database. This correspondence supports the morphotype identification of the individuals as *A. caliginosa*. For *O. lacteum*, a set of successfully amplified product sequences clustered with *O. lacteum* COI sequences available from BOLD within the constructed phylogenetic tree, supporting the morphological identification for these individuals (Supplementary Fig. 2). For a remaining set of *O. lacteum* individuals (38 of 72 individuals), amplification of the COI gene failed, despite best efforts to optimize primers and reaction conditions for PCR. Hence, support for the morphospecies identification for these individuals was not achieved through COI sequencing (see methods). Fortunately, the nuclear genomic loci analysed using the meAFLP method could, however, be used to confirm species identity for these individuals (see below).

Soil analysis and dosimetry modeling

Measured soil ^{137}Cs, ^{90}Sr, ^{241}Am and Pu-total, and earthworm gut ^{137}Cs were close to or below detection limits in all control sites and were highest at the H1 Glubokya Marsh site (Table 2). For modeling the transfer of radionuclides to earthworm tissues at CEZ sites, the external irradiation

348 from ^{137}Cs dominates the exposure profile independent of site (Fig. 1), with internal ^{241}Am
349 representing the next largest dose rate contributor (assuming a radiation weighting factor of 10).
350 The contribution of radionuclides to dose rates were similar across sites (e.g. Fig. 1a/b). Total
351 median modeled dose rates projected for earthworms across the gradient of sites ranged from
352 0.09 to 45 µGy/h, these values being correlated the with ambient dose rates, albeit at a factor of
353 2-3 times higher. The quoted internal dose rates represent only the contribution from actual
354 transfer across the gut or skin to the tissues, although the soil in the gut will act as an additional
355 source of exposure. For ^{137}Cs, this consideration makes little difference to the total dose rate
356 experienced. There could be a localised dose from ^{90}Sr to the gut surface, but within one order of
357 magnitude of the estimated internal dose rate, although localised dose may be similar. The
358 dominance of external exposure due to ^{137}Cs and the relative contributions of the different
359 radionuclides to internal dose are in agreement with dose estimates based upon radionuclide
360 activity concentrations measured in earthworms (Lumbricidae) and soil sampled from the Red
361 Forest (CEZ) in 2014 (Beresford et al., 2019a).
362
363 Earthworm size has a relatively small influence on modeled dose rates, with slightly lower ^{90}Sr
364 dose rates in small earthworms, which is expected from differences in absorption and attenuation.
365 At the most highly contaminated sites (H1 Glubokya Marsh), measured activity concentrations in
366 the gut soil of individual earthworms (29 - 53 Bq/g) showed good agreement with the levels
367 measured in the top 10 cm of soil (49 - 86 Bq/kg). These observations support the modeling
368 predictions that individuals at this site are more highly exposed than earthworms from the other
369 sampled locations.
370
371 Site soil pH range from mildly acidic (4.67) at the H1 Glubokya Marsh site with the highest
372 earthworm dose rate to close to neutral (6.23 and 6.66) at two of the low dose rate sites (C1
373 Glinka, C3 Chernobyl Garden). Soils contained between 4.5 and 15.6% organic matter as
374 measured by loss on ignition, the site with the highest dose rate having the highest value which
375 was almost double that any other site (Table 2). The calculated dose rate was significantly

negatively correlated with soil pH (Pearson correlation -0.86, $p<0.02$) and positively correlated with soil loss on ignition (Pearson correlation 0.781, $p<0.05$), with soil pH and loss on ignition also significantly negatively correlated (Pearson correlation -0.78, $p<0.05$). When the highest dose rate site was removed from the data-set, there was no longer a significant correlation with either soil pH or loss on ignition ($p>0.05$) indicating the importance of the low pH and high loss on ignition values for the H1 Glubokya Marsh site in driving the significant relationships seen between the soil properties.

Genetic and epigenetic characterisation of earthworms

Genetic structure within the collected earthworms was assessed using the AFLP analysis for samples at the *Msp*I cleavage site for all sampled individuals. Two distinct groupings were identified based on the obtained profiles. One group (orange squares in Supplementary Fig. 1) comprised confirmed morphotype *A. caliginosa*. These individuals included earthworms collected predominantly from two low exposure sites - C2: Zamozhnya and C3: Chernobyl gardens and a single individual from medium exposure site M2: Forest Lake 2. Given the similarly low levels of exposure experienced by all but one of the *A. caliginosa*, we focussed our further analysis on *O. lacteum* for which individuals were available from a number of locations with different measured and modeled exposure dose rates. Nonetheless, the *A. caliginosa* data was still valuable for taxonomic assignment.

The remaining AFLP profiles (red circles and green triangles in Supplementary Fig. 1) comprise a single and distinct group within the PCoA plot separated from the *A. caliginosa* samples along PCoA1. This second set of profiles contains all individuals from morphotype *O. lacteum* for which COI sequencing gave both a best BLAST hit against an existing *O. lacteum* COI sequence and for which clustered with a known *O. lacteum* COI reference sequences (green triangle, Supplementary Fig. 1) and also those morphotype *O. lacteum* from which the COI loci could not be amplified and sequenced (red circles, Supplementary Fig. 1). Based on morphological similarity of the individuals to the COI loci confirmed *O. lacteum* and the clustering of the AFLP profiles with

404 those of the COI confirmed individuals in the PCoA plot, we conclude that all the amplified
405 individuals correspond to one or more clades of *O. lacteum* for which the used primer set does not
406 amplify the COI gene. As likely *O. lacteum*, we concluded that these individuals can be analysed
407 alongside the COI confirmed *O. lacteum* for the assessment of the genetic, epigenetic and
408 microbiome response to ionising radiation at CEZ sites. However, when assessing driver of
409 differences between profiles we used the two potential mitochondrial lineages as fixed factors
410 within ANOVAs of the PCoA scores.
411
412 The AFLP analysis based on *Msp*I cleavage site markers for all *O. lacteum* showed overlap of
413 profiles between replicate earthworms (Fig. 2). Analysis of PCoA 1 scores indicated a significant
414 site effect (GLM $F=7.95$, $p<0.001$), but not of *O. lacteum* mitochondrial strain (GLM, $F=0.02$,
415 $P>0.01$). Between site differences were found for earthworms from the 6.8 µGy/h site and all other
416 locations, with the exception of the 0.12 µGy/h site. The differences in AFLP profiles of earthworms
417 from intermediate dose rate sites compared to those from the higher and lower dose rate sites
418 suggests that exposure to ionising radiation is not the main driver of AFLP profile differences.
419
420 To assess DNA methylation patterns in sampled *O. lacteum,* a second AFLP analysis was
421 conducted using the methylation sensitive *Hpa*II restriction enzyme. The meAFLP indicated an
422 average of 20.1% of methylation sensitive loci. DNA methylation levels showed no trend of hyper-
423 or hypo-methylation across sites (lowest average 16.7% at an exposure level of 0.12 µGy/h,
424 highest average 23.4% at an exposure level of 9.1 µGy/h, Fig. 3a). Principle coordinate analysis
425 of obtained methylation patterns indicated no site-specific structure among the profiles. Sampled
426 individuals showed no segregation within the PCoA on either of the first two principal coordinate
427 axes, which together account for only 20.6% of variance (Fig. 3b). No significant differences in
428 PCoA 1 or PCoA 2 scores were evident (PCoA 1 ANOVA $F=2.09$, $p>0.05$; PCoA 2 ANOVA $F=1.08$,
429 $p>0.05$). Consistent methylation levels and the overlap of methylation patterns among earthworms
430 sampled from sites with different radiation dose rates, suggests no effects of radiation exposure
431 on global DNA methylation patterns at CEZ sites for *O. lacteum*.

Sequencing of the 16S rRNA loci amplified from *O. lacteum* gut DNA identified 18870 OTUs at the 97% similarity threshold. An NMDS analysis using data for sequences allocated to these OTUs for each earthworm microbiome indicated a clear segregation of all individuals from each site within an NMDS analysis plot (Fig. 4). NMDS1 and NMDS2 scores were significantly correlated with median dose rate, soil pH and soil loss on ignition in all cases ($p<0.001$ all cases). However, due to the small number of sites, such correlations with average dose rate may be a potential artifact due to co-correlation effects. For this reason, to determine whether a given environmental variable may be a driver of microbiome change, we assessed the structure or this relationship – notably the monotonic nature of the response (i.e. score increase or decrease progressively in relation to environmental variable level). This site based separation by OTU profiles, did not show a monotonic relationship with radiation exposure level along the NMDS 1 axis, with low exposure level and high exposure levels sites having high NMDS 1 scores and medium exposure sites low values (Supplementary Fig. 3A). There was also a non-monotonic relationship of NMDS 1 score with site soil pH, the highest axis values found for the sites with the most acidic and alkaline soils (Supplementary Fig. 3B). There was an approximate monotonic relationship of NMDS 1 score with site soil loss on ignition (Supplementary Fig. 3C), indicating that soil organic matter composition may act as a critical driver of soil bacterial community structure either directly or through indirect effects on other soil properties such as water holding capacity which may affect soil responses to drought or frost. NMDS 2 score was close to monotonic related to calculated dose rate (Supplementary Fig. 3D). However, as there is co-correlation of the environmental drivers, both soil pH and loss on ignition also show a monotonic relationship with NMDS 2 score (Supplementary Fig. 3E and 3F).

Diversity expressed as Fishers log alpha was highest in the bacterial gut microbiome samples in *O. lacteum* earthworms from the two lowest exposure sites (C1 Glinka, C4 Marsh) and lowest in the two highest exposure sites (H1 Glubokya Marsh, M2 Forest Lake). Diversity increased systematically with increasing median earthworm dose rate (Fig. 5A). As pH is strongly co-

correlated with earthworm dose rate, there is also a relationship of increasing diversity at high soil pH values. Diversity was not systematically related to soil loss on ignition, with high diversity at both intermediate and high soil loss on ignition sites (Fig. 5B).

464 ***Discussion***

465 The scale and devastating nature of the Chernobyl accident has created a legacy of exposure for
466 wildlife living around the site of the former power plant. Radioecologists have studied the long-
467 term effects of the resulting exposure, both to support local management and to better understand
468 any long-term effects on individuals, populations, and ecosystems. Comprehensive reviews of the
469 phenotypic effects observed in wildlife experiencing prolonged exposure to elevated radionuclide
470 levels in the CEZ have highlighted the range of studies on the structure and function of exposure
471 populations and communities from soil microbial communities to charismatic vertebrate wildlife
472 (e.g. Beresford et al., 2016; Geras'kin et al., 2008; Hinton et al., 2007; Lourenco et al., 2016;
473 Steinhauser et al., 2014). Within the range of published studies, there is a lack of consensus on
474 the long-term effects of chronic radiation exposure for wildlife in the CEZ (Beresford et al., 2019b).
475 The impacts of radiation exposure on the hologenome and subsequent impacts on exposure and
476 subsequent generations have been identified as one factor that may contribute to the impacts of
477 long-term exposure in the CEZ (Horemans et al., 2019). Understanding such effects may benefit
478 from addressing uncertainties relating to the chronic effects of radiation exposure.

479

480 The prolonged exposure of soil invertebrates to long-lived contaminants has been shown to
481 change population genetic and epigenetic traits that underpin the development of tolerance
482 (Horemans et al., 2019). The relatively high reproductive rate of many invertebrates enables rare
483 or novel gene variants associated with adaptive traits to spread relatively quickly throughout
484 populations under selection pressure. Many invertebrates have been shown to develop adaptation
485 to contaminants (Klerks & Weis 1987; Posthuma & Van Straalen 1993). For earthworms, tolerance
486 to metal exposure has been shown in populations inhabiting sites polluted with a number of
487 different metals. Andre et al. (2010) used genetic marker analysis to identify an 'ecological island'
488 with little genetic overlap in *L. rubellus* populations inhabiting lead polluted and clean soils under
489 different pH conditions. Mutations in the Ca-transport gene SERCA were found between
490 populations, identifying this locus as a possible mechanism for adaptation. Langdon et al. (1999)
491 also working with *L. rubellus* found that individuals inhabiting two mining areas heavily polluted

with arsenic and copper (Devon Great Consols, Carrock Fell) could survive in arsenic-spiked soil that was acutely toxic to earthworms from an uncontaminated location. This tolerance was preserved following culturing over two generations, suggesting a genetic basis for the adapted phenotype (Langdon et al., 2009). Kille et al. (2013) used mitochondrial (COI) marker analysis and meAFLP to assess the genetic and epigenetic traits of *L. rubellus* from the same Devon Great Consols mine site studied by Langdon et al. (2009). Both the COI analysis and AFLP markers identified two genetic lineages of *L. rubellus* at the mine site consistent with previous findings (Anderson et al., 2017; Giska et al., 2015; Spurgeon et al., 2016). For the most genetically diverse lineage (A), segregation of local collection site populations by AFLP profiles was seen. For the second, less diverse, lineage (B), this genetic segregation by AFLP profile was not seen, however, site segregation by meAFLP profiles was observed. This indicates a contribution of the epigenome to the observed adaptive phenotype in Lineage B *L. rubellus*. This unique finding indicates the need to assess how both genetic sequence changes and DNA methylation can play a role in the development of adaptive phenotypes in earthworms.

An initial survey of Chernobyl earthworm communities identified that species are patchily distributed across the exclusion zone. The dominant soil type in the region is sandy in nature with characteristically low pH and organic matter content. Such free draining acid soils have been found to be poorly suited for earthworms, which maintain larger and more diverse communities in areas with high clay or silt content, high water holding capacity and high electrical conductivity (Nuutinen et al., 1998; Valckx et al., 2009). The main locations from which earthworms were collected were associated either with water bodies (lake or river margins, marshland) or improved soils managed as domestic gardens in areas of past human habitation. This indicates that soil hydrological status acts as a major driver of earthworm distributions within the CEZ.

Two species of earthworms were found in sufficient numbers to provide potential samples for analysis. Both *O. lacteum* and *A. caliginosa* are endogeic species that live in the mineral soil layers. Exposure in this habitat would be lower than to epigeic species living in the top-soil, since

almost 20 years after the accident, radionuclides remain largely in the upper 0-20 cm soil layers (Almgren and Isaksson, 2006; Ivanov and Kashparov, 2003). However, at the soil sampling depth used (10 cm), calculated dose rates would be generally representative for species living within the mineral soil layer. The individual measurements of relevant external and internal radionuclide concentrations for dosimetry assessment confirmed this exposure. Among the earthworms species found during the preliminary survey and main field sampling campaign, only *O. lacteum* was found in sufficient number across CEZ sites with comparatively low, medium and high exposure. *O. lacteum* is an endogeic earthworms species that is able to undertake both sexual and parthenogenetic reproduction, which may be relevant both for its relative prevalence in the CEZ and also potentially for its adaptation to local environmental conditions. *A. caliginosa*, another albeit larger endogeic earthworm species, was in contrast collected only from sites with near background levels. Too few sites were sampled to attribute the absence of *A. caliginosa* to the prevailing exposure levels. Absence is likely to be explained simply by the lack of suitable habitat for this species at the more contaminated sites.

Our analysis of the *O. lacteum* hologenome included measurement of genetic, epigenetic and microbiome characteristics. However, while covering key aspects, not all hologenome traits were included. For example in assessing epigenome responses, we focussed on an established method to measure coarse DNA methylation coverage. These DNA methylation marks were not mapped to genomic locations to provide insights in their functional role in gene regulation. Further, other potential epigenetic changes linked to the modification of histone protein and expression of regulatory microRNAs were not measured. These epigenome components have previously been found to be active in earthworms (Gong et al., 2010; Novo et al., 2015). Hence, their future inclusion within a more complete assessment of hologenome responses to ionising radiation exposures may be warranted.

The genetic analysis of *O. lacteum* using AFLP markers at *Msp*I restriction sites indicated that all morphotype earthworm from this species exist as a single group. Using the COI primers,

548 sequences from 53% of all collected morphotype *O. lacteum* failed to amplify despite best efforts.
549 The reasons for this failure are currently not clear, but may be related to the presence of specific
550 point sequence variations in the primer binding region of the COI sequence in these individuals.
551 The presence of these polymorphisms may be indicative of the cryptic mitochondrial lineages in
552 this species, as has been found for *O. lacteum* (Klarica et al., 2012) and also commonly for other
553 earthworm including *L. rubellus* (Anderson et al., 2017; Andre et al., 2010), *Eisenia fetida*
554 (PerezLosada et al., 2009) and *Allolobophora chlorotica* (King et al., 2008). The more
555 comprehensive AFLP data, however, refutes the presence of cryptic *O. lacteum* species, as the
556 PCoA analysis of the AFLP data shows that CEZ *O. lacteum* comprise a single clade.
557
558 Site-specific structure was observed within the *Msp*I restriction site AFLP analysis. This was not,
559 however, correlated with modeled earthworm dose rate. This suggests that there has been no
560 selection relating to the ionising radiation exposure. Similarly, we found no difference in DNA
561 methylation levels or structure within the meAFLP analysis, indicating that there is no site, and
562 hence ionising radiation exposure level, influence on the distribution of DNA methylation within the
563 *O. lacteum* genome. Many contaminants have been shown to alter gene methylation patterns in
564 invertebrates (Santoyo et al., 2011) and plants (Chinnusamy and Zhu, 2009). In response to
565 ionising radiation exposure in the CEZ, hypermethylation of DNA has been observed in pine trees
566 (*Pinus sp*.) and *Arabidopsis thaliana* (Kovalchuk et al., 2004; Kovalchuk et al., 2003) and it has
567 been suggested that individuals of adult pale blue grass butterfly *Zizeeria maha* at Fukahima have
568 shown inherited abnormalities from the F1 to the F2 generation (Hiyama et al., 2012). Epigenetic
569 mechanisms were proposed to play a role in both cases. Absence of a clear indication of changes
570 in patterns of DNA methylation measured using meAFLP for *O. lacteum* may indicate that adaptive
571 phenotypes may be regulated through other epigenome components. Alternatively, it is possible
572 that exposure at the sampled CEZ sites is not sufficient to cause significant epigenetic changes in
573 this species. However, in this context, it is important also to consider that meAFPL provides only
574 a very course assessment of one aspect of the response to the epigenome to perturbations. Other
575 methods for quantifying DNA methylation targeting either speciifc genes through methylation-

specific PCR or genome wide methylation analysis using high throughput sequencing approaches may better resolve any specific DNA methylation changes resulting from radiation exposure. Further, there are other epigenetic mechanisms that may also play a role.

The analysis of the structure of the CEZ *O. lacteum* microbiome indicated clear site structure in the composition of gut bacteria as analysed using 16S RNA gene loci amplification and sequencing. The earthworm microbiome has previously been found to be shifted in response to the presence of arsenic in contaminated soils at a mine site (Pass et al., 2015). In this study, the earthworm-associated microbiome was found to differ from the surrounding environment. Several taxa observed in uncontaminated control microbiomes were found to be suppressed by metal/metalloid field exposure, including the eradication of the hereto ubiquitously associated Verminephrobacter symbiont, which raises implications to its functional role in the earthworm microbiome (Pass et al., 2015).

It has been shown that the earthworm gut bacterial microbiome is a combination of soil associated species passing through the gut and also a range of strongly host related core species present across different soils (Liu et al., 2018; Pass et al., 2015). As the earthworms sampled in this survey were not starved or washed to remove soil in the gut, both core *O. lacteum* and also soil associated species would be present. Microbiome structure and diversity was systematically related to site soil properties. Analyses through 16s rRNA sequencing have indicated that soil properties can significantly affect the bacterial community (George et al., 2019; Plassart et al., 2019). Griffiths et al. (2011) showed that pH was a dominant driver of national patterns of soil bacterial species distribution, with other environmental variables and climatic variables and spatial correlations at local scale also influencing community structure. Given that the soil bacterial community contributes a significant proportion of earthworm microbiome species, the potential exists for soil properties to be responsible for differences in the microbiome.

603 *O. lacteum* gut bacterial microbiome structure was site specific and was weakly correlated with
604 dose rate. However, across sites there was also co-correlation between earthworm dose rates
605 and other soil properties, notably pH. Subtle shifts in soil bacterial community structure have
606 previously been shown to respond to radiation exposure, although at much higher dose rates than
607 those quantified here (Jones et al., 2004; McNamara et al., 2007; Niedree et al., 2013). Hence,
608 changes in earthworm gut microbiome structure and diversity may be related to soil dose rates.
609 However, the widely known role of soil pH as a driver of bacterial community structural difference
610 makes the attribution of the observed difference in microbiome structure to radiation exposure
611 challenging. Further, soil pH has been shown to be a key determinant of the speciation of metals
612 and radionuclides in soil (Lofts and Tipping, 2011; Vandenhove et al., 2007), with resulting effects
613 on bioavailability (Hegazy et al., 2013; Spurgeon et al., 2006). Hence, as well as the potential
614 direct effects of radionuclide and pH, there may be interactive pH effects on radionuclide
615 bioavailability which may complicate the attribution of *O. lacteum* gut bacterial community variation
616 to any single driver.
617
618 ***Conclusions***
619 Prevailing habitat, soil and climatic conditions mean that the distribution of earthworms in the CEZ
620 is spatially limited. Our survey suggests that earthworms are restricted to sites associated with
621 water bodies and in abandoned urban gardens. Our hologenome analyses indicate that there is
622 no major impact of the prolonged exposure of earthworms to radionuclides on the measured
623 genetic or epigenetic characteristics of earthworms collected across our studied sites. Earthworm
624 gut bacterial microbiome community did show strong site specific structure that could be related
625 to the prevailing dose rate predicted for earthworms living at each site. Co-correlation of other soil
626 properties with dose rate and potential interactions, however, means that it is not possible to
627 attribution of these changes specifically to radionuclide exposure. A wider survey is needed to
628 more robustly address questions relating to the impacts of radionuclide exposure on the
629 microbiome. Due to their limited distribution in the CEZ earthworm may not be the best study group
630 for such an extended survey. Robust wide-scale microbiome community structure is a potentially

631 effective approach, although it is acknowledged that microbe may be among some of the most
632 radio insensitive groups of organisms, the interplay between host health and microbiome structure
633 may indicate a wider interaction at the level of the hologenome.

Acknowledgments

This work was supported by the EU H2020 COMET (Coordination and implementation of a pan-European instrument for radioecology) research project (grant number: Fission-2012-3.4.1-604794), by NERC National Capability funding to the Centre for Ecology and Hydrology under the Institutional fund IMP scheme for D. Spurgeon, and the Norwegian Research Council CERAD project (grant number: 223268/F50). Greg Lamarre from the Czech Academy of Sciences was a part of the expedition team and contributed to the field collection.

643 ***References***

644

645 Almgren, S., Isaksson, M., 2006. Vertical migration studies of Cs-137 from nuclear weapons
646 fallout and the Chernobyl accident. Journal of Environmental Radioactivity 91, 90-102.

647

648 Anderson, C., Cunha, L., Sechi, P., Kille, P., Spurgeon, D., 2017. Genetic variation in populations
649 of the earthworm, *Lumbricus rubellus*, across contaminated mine sites. Bmc Genetics 18, 97.

650

651 Andre, J., King, R.A., Stürzenbaum, S.R., Kille, P., Hodson, M.E., Morgan, A.J., 2010. Molecular
652 genetic differentiation in earthworms inhabiting a heterogeneous Pb-polluted landscape.
653 Environmental Pollution 158, 883-890.

654

655 Beresford, N.A., Barnett, C.L., Gashschak, S., Maksimenko, A., Guliaichenko, E., Wood, M.D.,
656 Izquierdo, M., 2019a. Radionuclide transfer to wildlife at a 'Reference Site' in the Chernobyl
657 Exclusion Zone and resultant radiation exposures. Journal of Environmental Radioactivity,
658 105661. https://doi.org/105610.101016/j.jenvrad.102018.105602.105007.

659

660 Beresford, N.A., Fesenko, S., Konoplev, A., Skuterud, L., Smith, J.T., Voigt, G., 2016. Thirty years
661 after the Chernobyl accident: What lessons have we learnt? Journal of Environmental Radioactivity
662 157, 77-89.

663

664 Beresford, N.A., Scott, E.M., Copplestone, D., 2019b. Field effects studies in the Chernobyl
665 Exclusion Zone: Lessons to be learnt. Journal of Environmental Radioactivity, 1055893.

666

667 Bonzom, J.M., Hattenschwiler, S., Lecomte-Pradines, C., Chauvet, E., Gaschak, S., Beaugelin-
668 Seiller, K., Della-Vedova, C., Dubourg, N., Maksimenko, A., Garnier-Laplace, J., Adam-

669 Guillermin, C., 2016. Effects of radionuclide contamination on leaf litter decomposition in the
670 Chernobyl exclusion zone. Science of the Total Environment 562, 596-603.
671
672 Bordenstein, S.R., Theis, K.R., 2015. Host biology in light of the microbiome: Ten principles of
673 holobionts and hologenomes. PLOS Biology 13.
674
675 Boubriak, II, Grodzinsky, D.M., Polischuk, V.P., Naumenko, V.D., Gushcha, N.P., Micheev, A.N.,
676 McCready, S.J., Osborne, D.J., 2008. Adaptation and impairment of DNA repair function in pollen
677 of *Betula verrucosa* and seeds of *Oenothera biennis* from differently radionuclide-contaminated
678 sites of Chernobyl. Annals of Botany 101, 267-276.
679
680 Brown, J.E., Alfonso, B., Avila, R., Beresford, N.A., Copplestone, D., Prohl, G., Ulanovsky, A.,
681 2008. The ERICA Tool. Journal of Environmental Radioactivity 99, 1371-1383.
682
683 Chinnusamy, V., Zhu, J.K., 2009. Epigenetic regulation of stress responses in plants. Current
684 Opinion in Plant Biology 12, 133-139.
685
686 Darriba, D., Taboada, G.L., Doallo, R., Posada, D., 2012. jModelTest 2: more models, new
687 heuristics and parallel computing. Nature Methods 9, 772-772.
688
689 DeSantis, T.Z., Hugenholtz, P., Larsen, N., Rojas, M., Brodie, E.L., Keller, K., Huber, T., Dalevi,
690 D., Hu, P., Andersen, G.L., 2006. Greengenes, a chimera-checked 16S rRNA gene database and
691 workbench compatible with ARB. Applied and Environmental Microbiology 72, 5069-5072.
692
693 Dubois, C., Pophillat, M., Audebert, S., Fourquet, P., Lecomte, C., Dubourg, N., Galas, S., Camoin,
694 L., Frelon, S., 2019. Differential modification of the *C. elegans* proteome in response to acute and

chronic gamma radiation: Link with reproduction decline. Science of the Total Environment 676, 767-781.

Edwards, C.A., 2004. Earthworm Ecology, 2 ed. CRC Press, Boca Raton, Florida, USA, p. 441.

Egorova, A.S., Gessler, N.N., Ryasanova, L.P., Kulakovskaya, T.V., Belozerskaya, T.A., 2015. Stress resistance mechanisms in the indicator fungi from highly radioactive Chernobyl zone sites. Microbiology 84, 152-158.

Fisker, K.V., Holmstrup, M., Sorensen, J.G., 2013. Variation in metallothionein gene expression is associated with adaptation to copper in the earthworm Dendrobaena octaedra. Comparative Biochemistry and Physiology C-Toxicology & Pharmacology 157, 220-226.

Folmer, O., Black, M., Hoeh, W., Lutz, R., Vrijenhoek, R., 1994. DNA primers for amplification of mitochondrial cytochrome c oxidase subunit I from diverse metazoan invertebrates. Molecular Marine Biology and Biotechnology 3, 294-299.

George, P.B.L., Lallias, D., Creer, S., Seaton, F.M., Kenny, J.G., Eccles, R.M., Griffiths, R.I., Lebron, I., Emmett, B.A., Robinson, D.A., Jones, D.L., 2019. Divergent national-scale trends of microbial and animal biodiversity revealed across diverse temperate soil ecosystems. Nature Communications 10, 11.

Geras'kin, S.A., Fesenko, S.V., Alexakhin, R.M., 2008. Effects of non-human species irradiation after the Chernobyl NPP accident. Environment International 34, 880-897.

Giska, I., Sechi, P., Babik, W., 2015. Deeply divergent sympatric mitochondrial lineages of the earthworm *Lumbricus rubellus* are not reproductively isolated. BMC Evolutionary Biology 15, 217.

Gong, P., Xie, F.L., Zhang, B.H., Perkins, E.J., 2010. In silico identification of conserved microRNAs and their target transcripts from expressed sequence tags of three earthworm species. Computational Biology and Chemistry 34, 313-319.

Griffiths, R.I., Thomson, B.C., James, P., Bell, T., Bailey, M., Whiteley, A.S., 2011. The bacterial biogeography of British soils. Environmental Microbiology 13, 1642-1654.

Hegazy, A.K., Afifi, S.Y., Alatar, A.A., Alwathnani, H.A., Emam, M.H., 2013. Soil characteristics influence the radionuclide uptake of different plant species. Chemistry and Ecology 29, 255-269.

Hertel-Aas, T., Oughton, D.H., Jaworska, A., Bjerke, H., Salbu, B., Brunborg, G., 2007. Effects of chronic gamma irradiation on reproduction in the earthworm *Eisenia fetida* (Oligochaeta). Radiation Research 168, 515-526.

Hinton, T.G., Alexakhin, R., Balonov, M., Gentner, N., Hendry, J., Prister, B., Strand, P., Woodhead, D., 2007. Radiation-induced effects on plants and animals: Findings of the united nations Chernobyl forum. Health Physics 93, 427-440.

Hiyama, A., Nohara, C., Kinjo, S., Taira, W., Gima, S., Tanahara, A., Otaki, J.M., 2012. The biological impacts of the Fukushima nuclear accident on the pale grass blue butterfly. Scientific Reports 2, 570.

746 Horemans, N., Spurgeon, D.J., Lecomte-Pradines, C., Saenen, E., Bradshaw, C., Oughton, D.,
747 Rasnaca, I., Kamstra, J.H., Adam-Guillermin, C., 2019. Current evidence for a role of epigenetic
748 mechanisms in response to ionizing radiation in an ecotoxicological context. Environmental
749 Pollution 251, 469-483.
750
751 Ivanov, Y.A., Kashparov, V.A., 2003. Long-term dynamics of the radioecological situation in
752 terrestrial ecosystems of the Chernobyl exclusion zone. Environmental Science and Pollution
753 Research, 13-20.
754
755 Jones, H.E., West, H.M., Chamberlain, P.M., Parekh, N.R., Beresford, N.A., Crout, N.M.J., 2004.
756 Effects of gamma irradiation on *Holcus lanatus* (Yorkshire fog grass) and associated soil
757 microorganisms. Journal of Environmental Radioactivity 74, 57-71.
758
759 Kille, P., Andre, J., Anderson, C., Ang, H.N., Bruford, M.W., Bundy, J.G., Donnelly, R., Hodson,
760 M.E., Juma, G., Lahive, E., Morgan, A.J., Sturzenbaum, S.R., Spurgeon, D.J., 2013. DNA sequence
761 variation and methylation in an arsenic tolerant earthworm population. Soil Biology &
762 Biochemistry 57, 524-532.
763
764 King, R.A., Tibble, A.L., Symondson, W.O.C., 2008. Opening a can of worms: unprecedented
765 sympatric cryptic diversity within British lumbricid earthworms. Molecular Ecology 17, 4684-
766 4698.
767
768 Klarica, J., Kloss-Brandstatter, A., Traugott, M., Juen, A., 2012. Comparing four mitochondrial
769 genes in earthworms - Implications for identification, phylogenetics, and discovery of cryptic
770 species. Soil Biology & Biochemistry 45, 23-30.
771

772 Kovalchuk, I., Abramov, V., Pogribny, I., Kovalchuk, O., 2004. Molecular aspects of plant
773 adaptation to life in the Chernobyl zone. Plant Physiology 135, 357-363.
774
775 Kovalchuk, O., Burke, P., Arkhipov, A., Kuchma, N., James, S.J., Kovalchuk, I., Pogribny, I.,
776 2003. Genome hypermethylation in Pinus silvestris of Chernobyl - a mechanism for radiation
777 adaptation? Mutation Research-Fundamental and Molecular Mechanisms of Mutagenesis 529, 13-
778 20.
779
780 Kozich, J.J., Westcott, S.L., Baxter, N.T., Highlander, S.K., Schloss, P.D., 2013. Development of
781 a dual-index sequencing strategy and curation pipeline for analyzing amplicon sequence data on
782 the MiSeq Illumina sequencing platform. Applied and Environmental Microbiology 79, 5112-
783 5120.
784
785 Krivolutsky, D.A., 1996. Soil fauna as bioindicator of radioactive pollution, in: vanStraalen, N.M.,
786 Krivolutsky, D.A. (Eds.). NATO Science Series Partnership Sub-series 2, Environmental Security
787 pp. 189-196.
788
789 Krivolutzkii, D.A., Pokarzhevskii, A.D., Viktorov, A.G., 1992. Earthworm populations in soils
790 contaminated by the Chernobyl Atomic Power-station accident, 1986-1988. Soil Biology &
791 Biochemistry 24, 1729-1731.
792
793 Langdon, C.J., Morgan, A.J., Charnock, J.M., Semple, K.T., Lowe, C.N., 2009. As-resistance in
794 laboratory-reared F1, F2 and F3 generation offspring of the earthworm *Lumbricus rubellus*
795 inhabiting an As-contaminated mine soil. Environmental Pollution 157, 3114-3119.
796

797 Langdon, C.J., Piearce, T.G., Black, S., Semple, K.T., 1999. Resistance to arsenic-toxicity in a
798 population of the earthworm *Lumbricus rubellus*. Soil Biology & Biochemistry 31, 1963-1967.
799
800 Langdon, C.J., Piearce, T.G., Meharg, A.A., Semple, K.T., 2003. Inherited resistance to arsenate
801 toxicity in two populations of *Lumbricus rubellus*. Environmental Toxicology and Chemistry 22,
802 2344-2348.
803
804 Lecomte-Pradines, C., Hertel-Aas, T., Coutris, C., Gilbin, R., Oughton, D., Alonzo, F., 2017. A
805 dynamic energy-based model to analyze sublethal effects of chronic gamma irradiation in the
806 nematode *Caenorhabditis elegans*. Journal of Toxicology and Environmental Health A 80, 830-
807 844.
808
809 Liu, D.F., Lian, B., Wu, C.H., Guo, P.J., 2018. A comparative study of gut microbiota profiles of
810 earthworms fed in three different substrates. Symbiosis 74, 21-29.
811
812 Lofts, S., Tipping, E., 2011. Assessing WHAM/Model VII against field measurements of free metal
813 ion concentrations: model performance and the role of uncertainty in parameters and inputs.
814 Environmental Chemistry 8, 501-516.
815
816 Lourenco, J., Mendo, S., Pereira, R., 2016. Radioactively contaminated areas: Bioindicator species
817 and biomarkers of effect in an early warning scheme for a preliminary risk assessment. Journal of
818 Hazardous Materials 317, 503-542.
819
820 Marinissen, J.C.Y., Vandenbosch, F., 1992. Colonization of new habitats by earthworms.
821 Oecologia 91, 371-376.
822

McMurdie, P.J., Holmes, S., 2013. Phyloseq: An R package for reproducible interactive analysis and graphics of microbiome census data. PLOS One 8.

McNamara, N.P., Griffiths, R.I., Tabouret, A., Beresford, N.A., Bailey, M.J., Whiteley, A.S., 2007. The sensitivity of a forest soil microbial community to acute gamma-irradiation. Applied Soil Ecology 37, 1-9.

Moller, A.P., Mousseau, T.A., 2009. Reduced abundance of insects and spiders linked to radiation at Chernobyl 20 years after the accident. Biology Letters 5, 356-359.

Nakamori, T., Yoshida, S., Kubota, Y., Ban-nai, T., Kaneko, N., Hasegawa, M., Itoh, R., 2008. Effects of acute gamma irradiation on Folsomia candida (Collembola) in a standard test. Ecotoxicology and Environmental Safety 71, 590-596.

Niedree, B., Berns, A.E., Vereecken, H., Burauel, P., 2013. Do Chernobyl-like contaminations with Cs-137 and Sr-90 affect the microbial community, the fungal biomass and the composition of soil organic matter in soil? Journal of Environmental Radioactivity 118, 21-29.

Novo, M., Lahive, E., Diez-Ortiz, M., Matzke, M., Morgan, A.J., Spurgeon, D.J., Svendsen, C., Kille, P., 2015. Different routes, same pathways: Molecular mechanisms under silver ion and nanoparticle exposures in the soil sentinel *Eisenia fetida*. Environmental Pollution 205, 385-393.

Nuutinen, V., Pitkanen, J., Kuusela, E., Widbom, T., Lohilahti, H., 1998. Spatial variation of an earthworm community related to soil properties and yield in a grass-clover field. Applied Soil Ecology 8, 85-94.

Ouellet, G., Lapen, D.R., Topp, E., Sawada, M., Edwards, M., 2008. A heuristic model to predict earthworm biomass in agroecosystems based on selected management and soil properties. Applied Soil Ecology 39, 35-45.

Pass, D.A., Morgan, A.J., Read, D.S., Field, D., Weightman, A.J., Kille, P., 2015. The effect of anthropogenic arsenic contamination on the earthworm microbiome. Environmental Microbiology 17, 1884-1896.

PerezLosada, M., Ricoy, M., Marshall, J.C., Dominguez, J., 2009. Phylogenetic assessment of the earthworm *Aporrectodea caliginosa* species complex (Oligochaeta: Lumbricidae) based on mitochondrial and nuclear DNA sequences. Molecular Phylogenetics and Evolution 52, 293-302.

Plassart, P., Prevost-Boure, N.C., Uroz, S., Dequiedt, S., Stone, D., Creamer, R., Griffiths, R.I., Bailey, M.J., Ranjard, L., Lemanceau, P., 2019. Soil parameters, land use, and geographical distance drive soil bacterial communities along a European transect. Scientific Reports 9.

Popic, J.M., Salbu, B., Skipperud, L., 2012. Ecological transfer of radionuclides and metals to free-living earthworm species in natural habitats rich in NORM. Science of the Total Environment 414, 167-176.

Posada, D., 2008. jModelTest: Phylogenetic model averaging. Molecular Biology and Evolution 25, 1253-1256.

Rognes, T., Flouri, T., Nichols, B., Quince, C., Mahe, F., 2016. VSEARCH: a versatile open source tool for metagenomics. Peerj 4.

875 Rusin, A., Lapied, E., Le, M., Seymour, C., Oughton, D., Haanes, H., Mothersill, C., 2019. Effect
876 of gamma radiation on the production of bystander signals from three earthworm species irradiated
877 in vivo. Environmental Research 168, 211-221.
878
879 Santoyo, M.M., Flores, C.R., Torres, A.L., Wrobel, K., Wrobel, K., 2011. Global DNA methylation
880 in earthworms: A candidate biomarker of epigenetic risks related to the presence of
881 metals/metalloids in terrestrial environments. Environmental Pollution 159, 2387-2392.
882
883 Sowmithra, K., Shetty, N.J., Harini, B.P., Jha, S.K., Chaubey, R.C., 2015. Effects of acute gamma
884 radiation on the reproductive ability of the earthworm Eisenia fetida. Journal of Environmental
885 Radioactivity 140, 11-15.
886
887 Spurgeon, D.J., Liebeke, M., Anderson, C., Kille, P., Lawlor, A., Bundy, J.G., Lahive, E., 2016.
888 Ecological drivers influence the distributions of two cryptic lineages in an earthworm
889 morphospecies. Applied Soil Ecology 108, 8-15.
890
891 Spurgeon, D.J., Lofts, S., Hankard, P.K., Toal, M., McLellan, D., Fishwick, S., Svendsen, C., 2006.
892 Effect of pH on metal speciation and resulting metal uptake and toxicity for earthworms.
893 Environmental Toxicology and Chemistry 25, 788-796.
894
895 Srut, M., Drechsel, V., Hockner, M., 2017. Low levels of Cd induce persisting epigenetic
896 modifications and acclimation mechanisms in the earthworm *Lumbricus terrestris*. PLOS One 12.
897
898 Steinhauser, G., Brandl, A., Johnson, T.E., 2014. Comparison of the Chernobyl and Fukushima
899 nuclear accidents: A review of the environmental impacts. Science of the Total Environment 470,
900 800-817.

Tindall, B.J., Rossello-Mora, R., Busse, H.J., Ludwig, W., Kampfer, P., 2010. Notes on the characterization of prokaryote strains for taxonomic purposes. International Journal of Systematic and Evolutionary Microbiology 60, 249-266.

Uematsu, S., Smolders, E., Sweeck, L., Wannijn, J., Van Hees, M., Vandenhove, H., 2015. Predicting radiocaesium sorption characteristics with soil chemical properties for Japanese soils. Science of the Total Environment 524, 148-156.

Valckx, J., Cockx, L., Wauters, J., VanMeirvenne, M., Govers, G., Hermy, M., Muys, B., 2009. Within-field spatial distribution of earthworm populations related to species interactions and soil apparent electrical conductivity. Applied Soil Ecology 41, 315-328.

Vandenhove, H., Van Hees, M., Wouters, K., Wannijn, J., 2007. Can we predict uranium bioavailability based on soil parameters? Part 1: Effect of soil parameters on soil solution uranium concentration. Environmental Pollution 145, 587-595.

Wang, Q., Garrity, G.M., Tiedje, J.M., Cole, J.R., 2007. Naive Bayesian classifier for rapid assignment of rRNA sequences into the new bacterial taxonomy. Applied and Environmental Microbiology 73, 5261-5267.

Xiong, L.Z., Xu, C.G., Maroof, M.A.S., Zhang, Q.F., 1999. Patterns of cytosine methylation in an elite rice hybrid and its parental lines, detected by a methylation-sensitive amplification polymorphism technique. Molecular & General Genetics 261, 439-446.

926 Zaitsev, A.S., Gongalsky, K.B., Nakamori, T., Kaneko, N., 2014. Ionizing radiation effects on soil
927 biota: Application of lessons learned from Chernobyl accident for radioecological monitoring.
928 Pedobiologia 57, 5-14.

Table 1. Site, habitat, number of earthworm species present and count of *A. caliginosa* and *O. lacteum* collected and thereafter treated as separate biological replicates from each collection location.

Site Number	Northing	Easting	Distance to Power Plant (km)	Habitat	Sample date	Species present	*Aporrectdea caliginosa*	*Octolasion lacteum*
C1 Glinka (4)	51.241295	29.9908887	18.3	Wetland margin	06/10/2016	5	0	3
C2 Zamozhnya (7)	51.236371	29.898201	20.7	Wetland margin	07/10/2016	4	13	0
C3 Chernobyl Garden (6)	51.279219	30.213228	14.5	Abandoned Garden	07/10/2016	3	18	0
C4 Marsh (9)	51.474772	29.633966	33.5	Marshland	10/10/2016	2	0	11
M1 Forest lake 1 (2)	51.41190	30.100092	2.6	Wetland margin	06/10/2016	2	0	27
M2 Forest lake 2 (3)	51.410225	30.100816	2.2	Wetland margin	06/10/2016	3	1	16
H1 Glubokya Marsh) (8)	51.445025	30.063611	6.5	Marshland	08/10/2016	2	0	13

Table 2. Site soil properties, measured radionuclide concentrations, modeled total earthworm and gut dose rates and median dose rate values (used for site labels) for all collection locations.

Site Number	Soil pH	Soil loss on ignition (%)	Measured surface dose rate (µGy/h)	Soil Bq/g ^{137}CS	Soil Bq/g ^{90}Sr	Soil Bq/g ^{241}Am	Soil Bq/g $^{total}Pu$	Earthworm dose rate range (µGy/h)	Worm gut activty Bq/g ^{137}Cs	Median worm dose rate for site (µGy/h)
C1 Glinka (4)	6.23	4.8	0.05 - 0.11	0.3	<0.48	0.003	<0.02	0.096 - 0.144	<2	**0.12**
C2 Zamozhnya (7)	5.87	8.5	0.1	0.2	<0.48	0.004	<0.02	0.072 - 0.108	<2	**0.09**
C3 Chernobyl Garden (6)	6.66	5.1	0.2	0.66	<0.48	0.02	<0.02	0.27 - 0.41	<2	**0.34**
C4 Marsh (9)	5.78	10.3	0.15 - 0.2	0.54	<0.48	0.01	<0.02	0.19 - 0.29	2.2+/-0.9	**0.24**
M1 Forest lake 1 (2)	5.73	4.5	2.8 - 3.5	10.1	20.3	0.54	0.18	6.12 - 7.48	NA	**6.8**
M2 Forest lake 2 (3)	5.49	6.1	7 - 8	16.9	7.1	0.59	0.33	8.2 - 10	NA	**9.1**
H1 Glubokya Marsh (8)	4.67	15.6	8 - 12	49 - 86	18 - 28	2.3 - 4.1	0.6 - 2.3	29 - 53	20 - 76	**45**

Legends to figures

Figure 1. Relative proportionate contribution of different measured radionuclides at sites with median ambient dose rates of 0.24 (Left pie chart) and 45 µGy/h (Right pie chart B) for earthworms sampled in the CEZ.

Figure 2. Principle coordinate analysis of *O. lacteum Msp*I AFLP multi-locus profiling collected at five sites in the CEZ with different soil total earthworm dose rates.

Figure 3. (Panel A) Percentage of methylated susceptible loci for *O. lacteum* collected at five sites in the CEZ with different soil total earthworm dose rates (µGy/h); and, (Panel B) principle coordinate analysis for *Msp*I/*Hpa*II meAFLP analysis for methylation loci for *O. lacteum Msp*I AFLP multi-locus profiling collected at five sites in the CEZ with different total soil earthworm dose rates.

Figure 4. Non-metric multidimensional scaling plot of 16S rRNA gene sequence analysis of gut microbiomes of *O. lacteum* collected at five sites in the CEZ with different total soil earthworm dose rates and the relationships with environmental vectors oriented in the direction of greatest increase with length is proportional to their correlation with the two NMDS axes.

Figure 5. Diversity of bacterial sequenced OTUs within the earthworm microbiome for *O. lacteum* collected from five locations within the CEZ expressed as Fischer's alpha in relation to soil (A) pH and (B) loss on ignition, bars are shaded according to earthworm dose rate (µGy/h).

Fig. 1

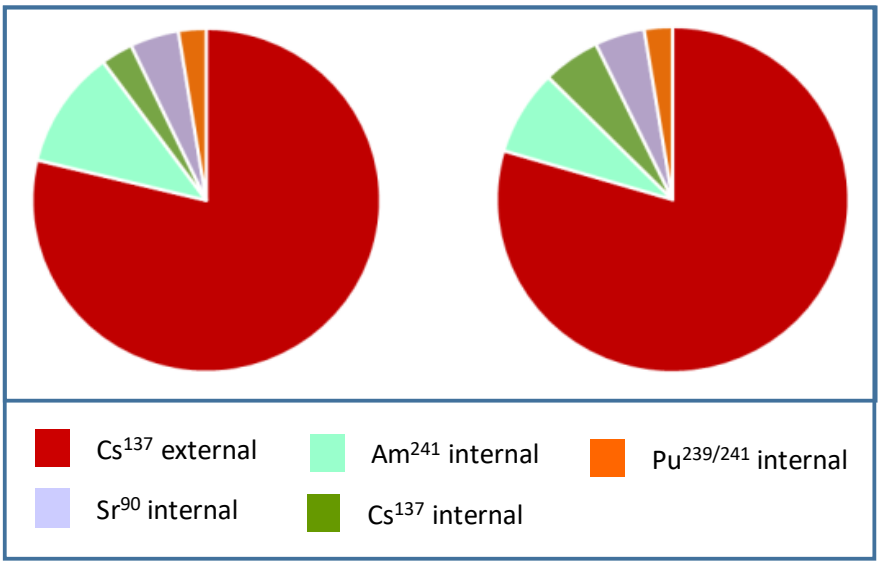
Cs137 external
Am241 internal
Pu239/241 internal
Sr90 internal
Cs137 internal

Fig. 2

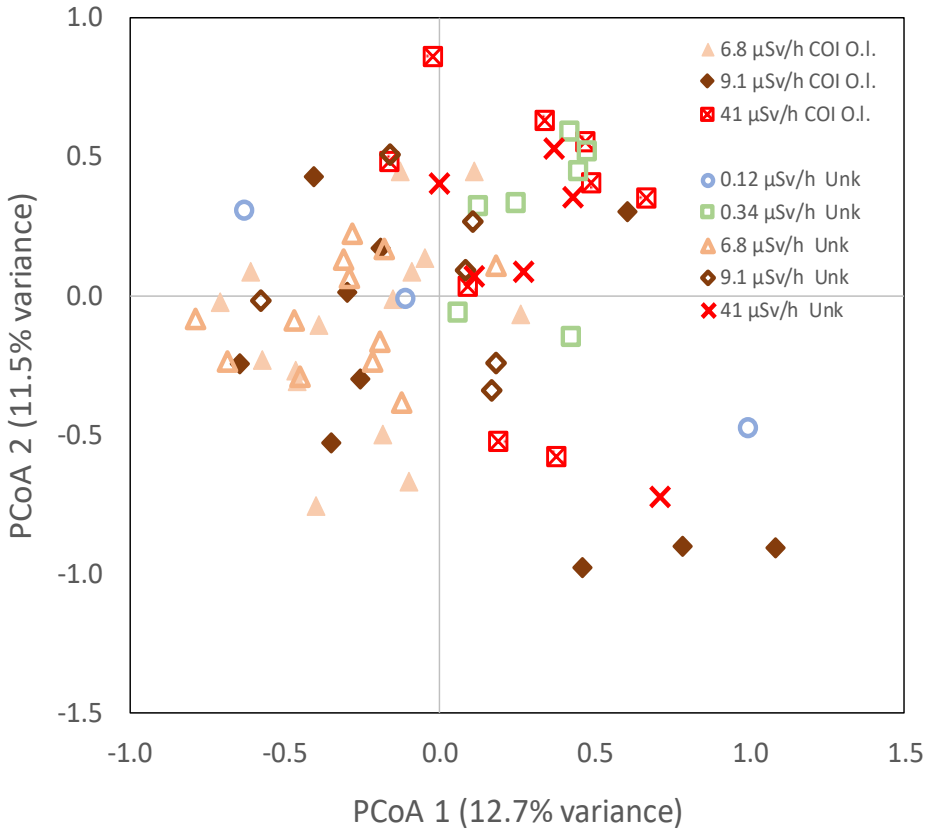
1.0
0.5
0.0
-0.5
-1.0
-1.5
-1.0
-0.5
0.0
0.5
1.0
1.5
PCoA 2 (11.5% variance)
PCoA 1 (12.7% variance)
6.8 µSv/h COI O.l.
9.1 µSv/h COI O.l.
41 µSv/h COI O.l.
0.12 µSv/h Unk
0.34 µSv/h Unk
6.8 µSv/h Unk
9.1 µSv/h Unk
41 µSv/h Unk

Fig. 3

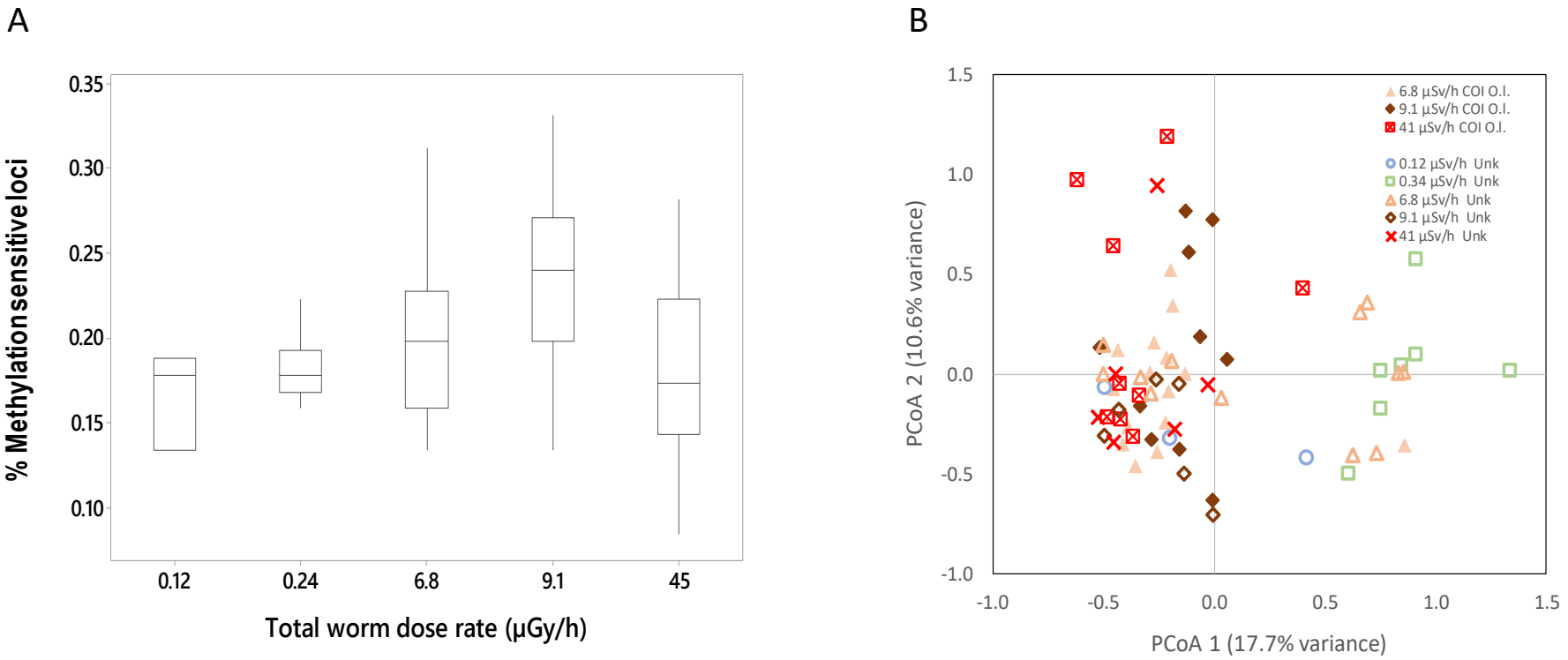
A
% Methylation sensitive loci
0.35
0.30
0.25
0.20
0.15
0.10
0.12
0.24
6.8
9.1
45
Total worm dose rate (µGy/h)
B
PCoA 2 (10.6% variance)
PCoA 1 (17.7% variance)
1.5
1.0
0.5
0.0
-0.5
-1.0
6.8 µSv/h COI O.I.
9.1 µSv/h COI O.I.
41 µSv/h COI O.I.
0.12 µSv/h Unk
0.34 µSv/h Unk
6.8 µSv/h Unk
9.1 µSv/h Unk
41 µSv/h Unk

Fig. 4

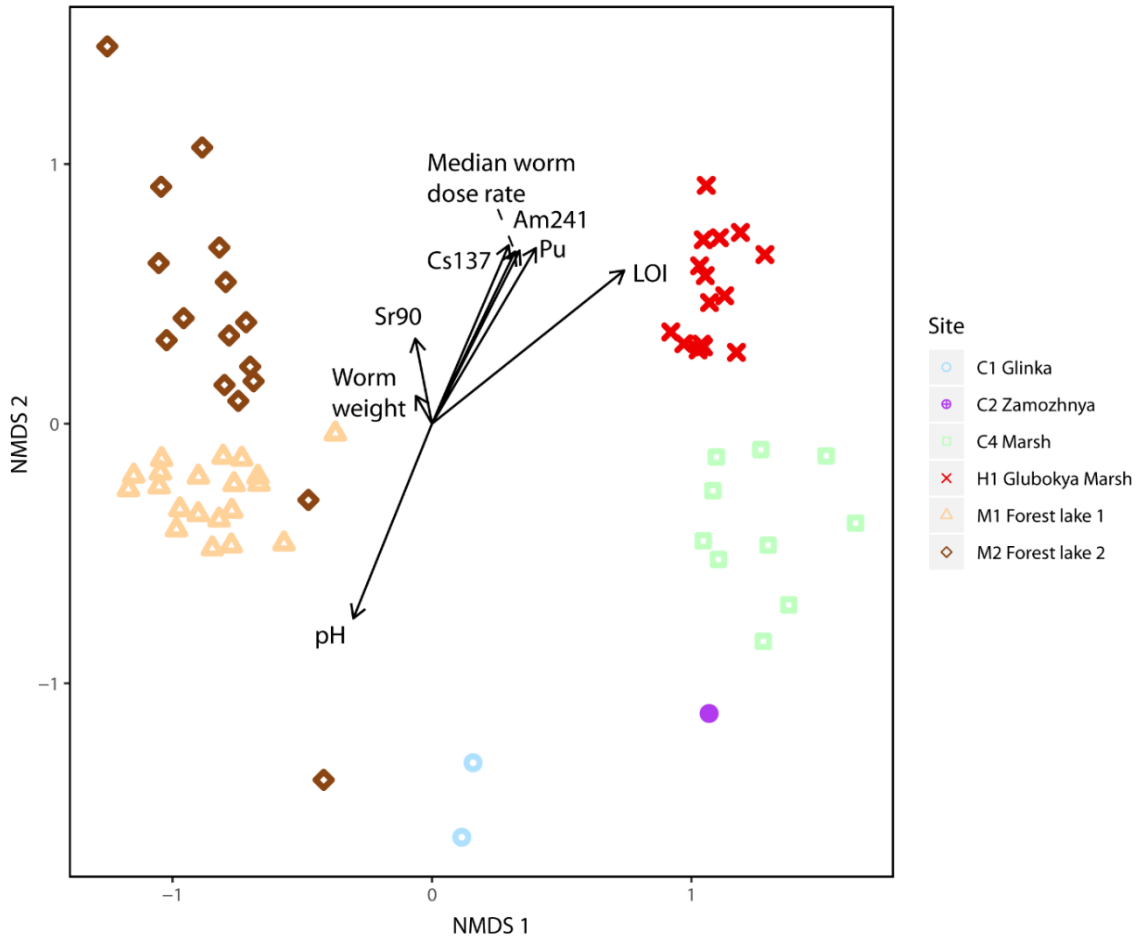
Median worm
dose rate
Am241
Cs137
Pu
LOI
Sr90
Worm
weight
pH
NMDS 1
NMDS 2
1
0
−1
−1
0
1
Site
C1 Glinka
C2 Zamozhnya
C4 Marsh
H1 Glubokya Marsh
M1 Forest lake 1
M2 Forest lake 2

Fig. 5

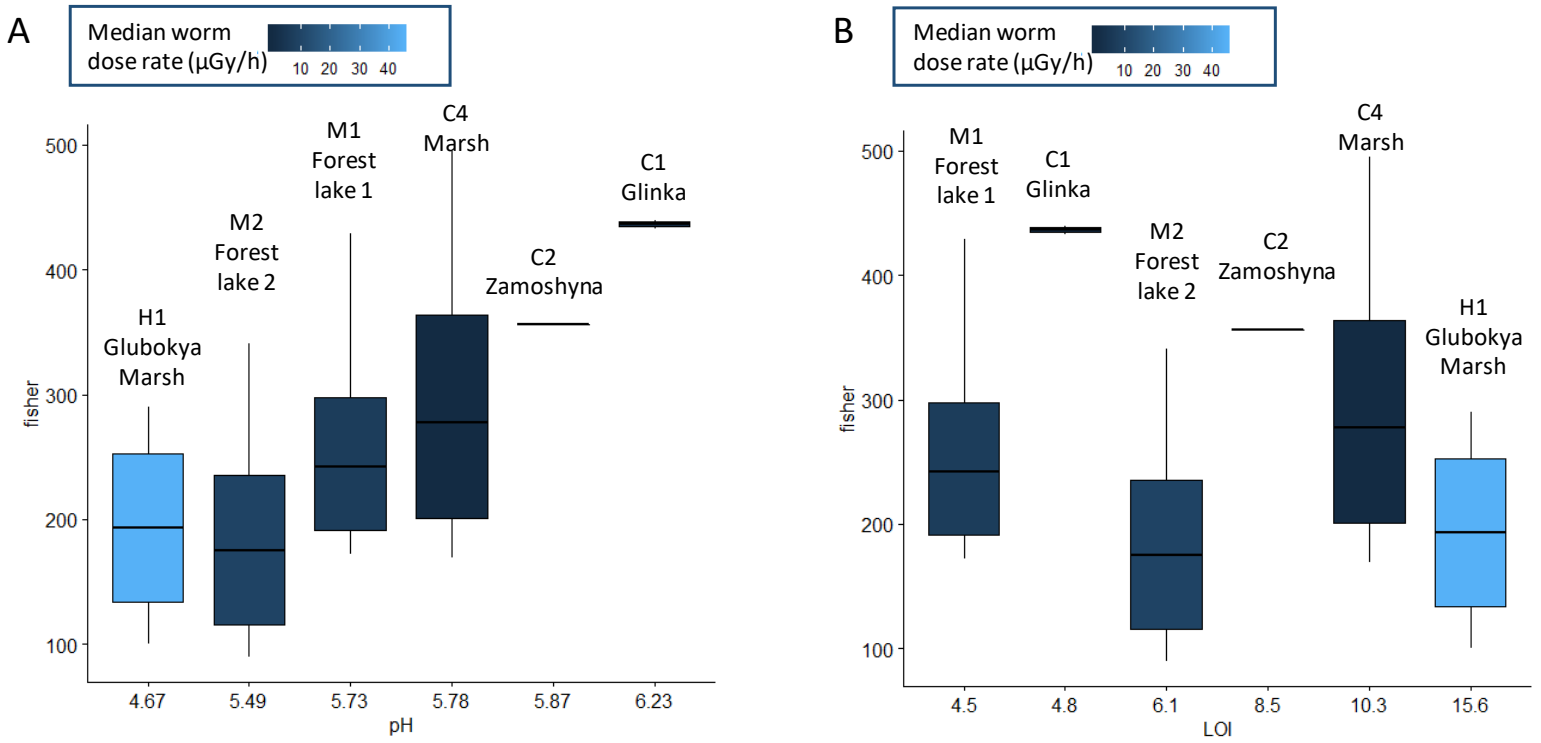
A
Median worm dose rate (µGy/h)
10 20 30 40
H1 Glubokya Marsh
M2 Forest lake 2
M1 Forest lake 1
C4 Marsh
C2 Zamoshyna
C1 Glinka
fisher
500
400
300
200
100
4.67
5.49
5.73
5.78
5.87
6.23
pH
B
Median worm dose rate (µGy/h)
10 20 30 40
M1 Forest lake 1
C1 Glinka
M2 Forest lake 2
C2 Zamoshyna
C4 Marsh
H1 Glubokya Marsh
fisher
500
400
300
200
100
4.5
4.8
6.1
8.5
10.3
15.6
LOI

Supplementary Figure 1. Principle coordinate analysis of AFLP *Msp*I multi-locus profiles for morphotype *O. lacteum* and *A. caliginosa*: morphotype *A. caliginosa* confirmed by COI sequencing cluster to the right; morphotype *O. lacteum* both confirmed by COI sequencing and which also fail to amplify for the COI locus cluster to the left as a single group.

Supplementary Figure 2. Phylogenetic gene tree showing the relationships between individual collected earthworms successfully amplified and sequenced for the Cytochrome oxidase I loci; branch distance indicates the degree of base substitutions between individual; all samples labeled starting P1 or P2 correspond to study samples with all other samples corresponding to reference specimen sequences.

Supplementary Figure 3. Relationship between NMDS axis 1 score and soil (A) median earthworm dose rate (µGy/h), (B) pH, (C) loss on ignition and NMDS axis 2 score and soil (D) median earthworm dose rate, (E) pH, (F) loss on ignition.